ORIGINAL RESEARCH

Poly(γ-Glutamic Acid)/Chitosan Hydrogel Nanoparticles For Effective Preservation And Delivery Of Fermented Herbal Extract For Enlarging Hair Bulb And Enhancing Hair Growth

Hye Su Kim [1]
Ha-Kyoung Kwon [2]
Dong Hoon Lee [1]
Thao Nguyen Le [1]
Hye-Jin Park [2]
Moon Il Kim [1]

[1]Department of BioNano Technology, Gachon University, Seongnam, Gyeonggi 13120, Republic of Korea; [2]Department of Food Science and Biotechnology, Gachon University, Seongnam, Gyeonggi 13120, Republic of Korea

Introduction: Hair growth-promoting herbal extract mixtures (4HGF) exhibits significant anti-inflammatory activities relevant to promoting hair growth; however, its efficacy in patients with hair loss has been limited majorly due to its low penetration ability into hair follicles. Herein, we prepared hydrogels via dropwise addition of poly(γ-glutamic acid) (PGA) solution containing 4HGF into chitosan (CS) solution, resulting in quick formation of ~400 nm-sized hydrogel particles through electrostatic interaction-derived ionic gelation with over 50% encapsulation efficiency of 4HGF (PGA-4HGF).

Methods: The size and morphology of PGA-4HGF were characterized by TEM, SEM, and dynamic light scattering analyses. Encapsulation efficiency and loading capacity of 4HGF within PGA-4HGF, as well as in vitro release profiles were determined by simply measuring the characteristic absorbance of 4HGF. Penetrating efficiency of PGA-4HGF was evaluated by tracking the respective fluorescence through model porcine skin with confocal laser microscope system. By treating PGA-4HGF on telogenic mice and dermal papilla cells (DPCs), we evaluated the size of hair bulbs in mice, as well as morphological changes in DPCs.

Results: Negligible and sustained release of entrapped 4HGF from the hydrogel nanoparticles were observed under acidic and physiological pH conditions, respectively, which is quite advantageous to control their release and prolong their hair growth-promoting effect. The hydrogel nanoparticles were penetrable through the porcine skin after incubation with or without shaking. After treating telogenic mice and DPCs with PGA-4HGF, we detected enlargement of hair bulbs and remarkable shape changes, respectively, thereby showing its potential in induction of hair growth.

Conclusion: These results suggest that the hydrogel nanoparticle formulation developed in this study can be employed as a potential approach for the preservation of hair growth-promoting compounds, their delivery of into hair follicles, and enhancing hair growth.

Keywords: hair growth, poly(γ-glutamic acid), chitosan, hydrogel nanoparticle, cosmeceutical

Correspondence: Moon Il Kim
Department of BioNano Technology, Gachon University, 1342 Seongnamdae-ro, Sujeong-gu, Seongnam, Gyeonggi 13120, Republic of Korea
Tel +82 31 750 8563
Fax +82 31 750 4748
Email moonil@gachon.ac.kr

Introduction

In the field of cosmetics or cosmeceuticals, it is believed that smaller particles are readily absorbed into the skin and function more efficiently. In this regard, nano-technology-derived materials may help develop many unique formulations with highly enhanced efficiency for penetrating through the skin, preserving activity with

prolonged effects, and additional advantageous features like delivering either hydrophobic or hydrophilic cosmeceutical compounds.[1] Diverse nanometer-sized materials have been reported so far, such as nanoemulsions, polymeric nanocapsules, liposome formulations, hydrogel nanoparticles, niosomes, nanocrystals, carbon nanoparticles, including carbon nanotubes or fullerenes, and dendrimers.[2] Among them, hydrogel-based delivery systems have gained particular attention due to their unique advantages of good air permeability across membrane and moisture retention, with the capacity for facile modification of surface and size.[3] Hydrogel nanoparticles can also be easily prepared through electrostatic interactions between polyelectrolytes without addition of toxic crosslinking chemicals. Poly(γ-glutamic acid) (PGA) is a natural anionic peptide, which exhibits good water solubility, biodegradability, and biocompatibility.[4] Chitosan (CS) is a natural polysaccharide, which preserves reactive hydroxyl and amino groups. CS has been also extensively applied in health/medical/pharmaceutical field, based on their excellent biocompatibility, biodegradability, antibacterial property, no cytotoxicity, high charge density, low cost, mucoadhesive and immunomodulating ability, with enhanced permeating property enabling to cross cellular membrane.[5,6] In acidic conditions, CS is protonated and becomes positively charged, so that it can form a hydrogel with polyanions, like sodium tripolyphosphate or PGA, via electrostatic interactions.[7,8] Based on these features of PGA and CS, nanometer-sized PGA/CS hydrogels were previously prepared for encapsulating several drug compounds for their efficient delivery.[3,8–11] Although the potential of PGA/CS nanoparticles has been demonstrated by several recent studies, further investigations are required to expand and widen their utility, which is currently limited to the biomedical field, majorly for drug delivery or wound dressing.

Hair care is a promising field for the cosmeceutical application of nanotechnology-derived materials.[12] Similar to skin or nail, hair is a keratinous filament made up with hair follicle and shaft.[13] Hair follicles are the pockets of the epidermis, which extend through most or all of the skin depth and enclose a small papilla of dermis at their base. The hair bulb formed at the base of the follicles is a structure of actively growing cells, consequently producing a long and fine cylinder of a hair.[14] Based on diverse studies of hair-growing mechanisms, many companies are currently using nanotechnology-based products and conducting further research to develop new products to enhance the shine,

silkiness, and health of hair, as well as to prevent hair loss and promote hair growth. In particular, the number of people suffering from hair loss is seriously increasing and the age of onset is gradually decreasing, mainly due to changes in dietary habits leading to nutritional imbalances, increased environmental pollution, and increased social stress, all of which can cause metabolic and hormonal disturbances, leading to hair loss.[15–17] As the FDA-approved drugs (minoxidil and propecia) have serious side effects, including erectile dysfunction with loss of libido,[18,19] there is an urgent need to develop more efficient hair growth-promoting agents, which are free from side effects and other toxic effects on humans. To meet this requirement, diverse agents derived from natural sources have gained attention due to their potential to promote hair growth without any serious toxicity.[20] Fermented herbal extract mixtures (4HGF) isolated from *Phellinus linteus* grown on germinated brown rice, *Cordyceps militaris* grown on germinated soybeans, and *Polygonum multiflorum, Ficus carica*, and *Cocos nucifera* oil show significant anti-inflammatory activities relevant to promoting hair growth.[21] However, until now, their efficacy in patients with hair loss has been limited majorly due to their low penetration ability into hair follicles.

Herein, we developed hydrogel nanoparticles composed of PGA and CS, which consist of hair growth-promoting 4HGF within the gel matrices (PGA-4HGF), to enhance the penetration efficiency of 4HGF, prolong its effects, and thus promote hair growth. PGA and CS were chosen as they can induce high electrostatic interaction between anionic PGA and cationic CS, yielding quick ionic gelation for the assembly of nanosized hydrogel particles with efficient entrapment of 4HGF.[3,9,11] We envisioned that the nanosized hydrogel formulation would serve as an efficient 4HGF delivery vehicle, thereby promoting hair growth. Specifically, when PGA-4HGF is applied on the human scalp, the nanoparticles are expected to penetrate the scalp barrier more efficiently than free 4HGF. Furthermore, after penetrating into the human follicles, sustained release of entrapped 4HGF might be triggered by the physiological pH environment. Hence, efficient 4HGF delivery can be achieved by utilizing PGA-4HGF (Figure 1). To prove the hypothesis, the size, surface charge, and morphological features of the hydrogels were characterized. Various in vitro characteristics of PGA-4HGF, including time-dependent release profiles, penetration efficiency in model porcine skin, and thermal stability were investigated. After treatment with PGA-4HGF, a remarkable change in the shape of dermal papilla
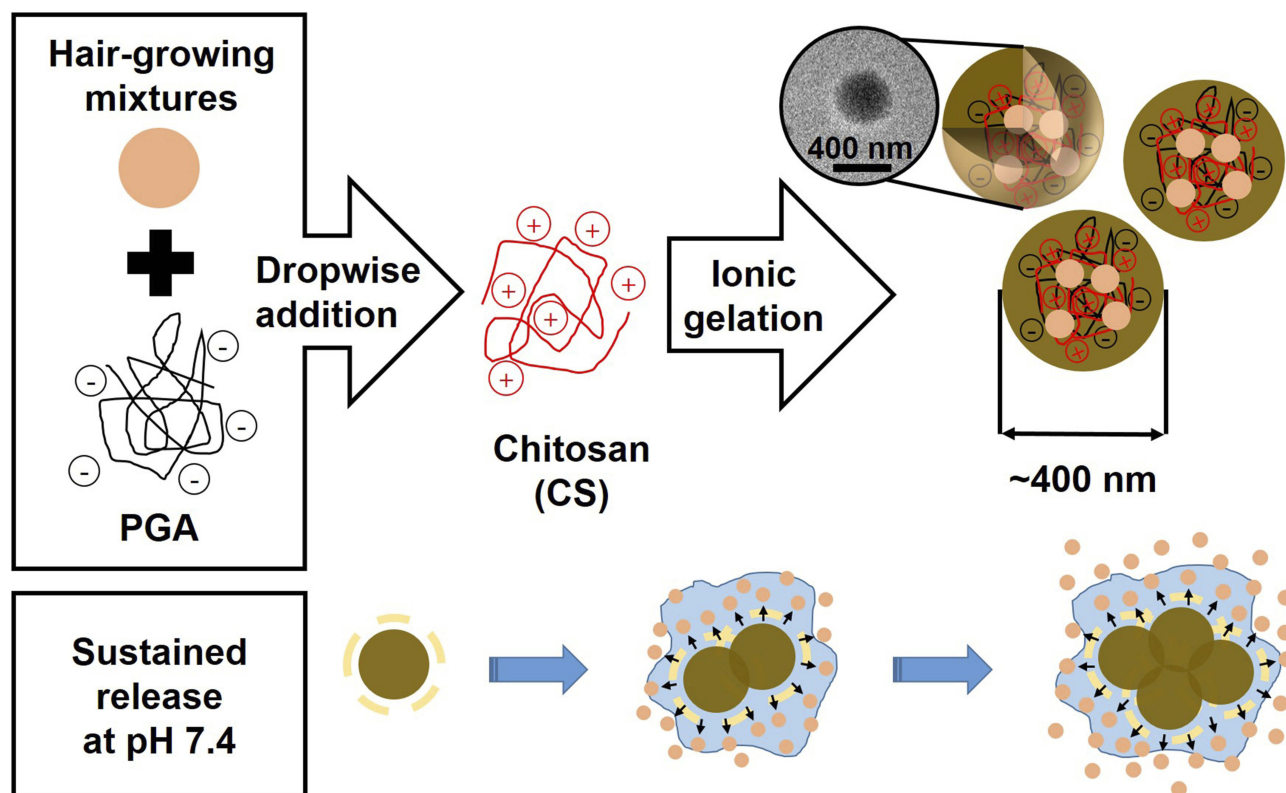
Figure 1 Schematic illustration of the synthesis of PGA-4HGF and its sustained release under physiological pH condition.

cells (DPCs) and larger hair bulbs in telogenic mice were observed, as compared to treatment with PGA-control without 4HGF or free 4HGF.

Materials And Methods
Materials
Crude 4HGF (the mixtures of *P. linteus* grown on germinated brown rice, *C. militaris* grown on germinated soybeans, and *P. multiflorum, F. carica*, and *C. nucifera* oil) was kindly provided by CARI Co. Ltd. Acetic acid, phosphate buffered saline (PBS), magnesium chloride, fluorescein isothiocyanate isomer I (FITC), and 2,2-diphenyl-1-picrylhydrazyl (DPPH) were purchased from Sigma-Aldrich (St. Louis, MO). PGA (molecular weight = 200,000–400,000) and CS (molecular weight = ~500,000) were purchased from Vedan Biotechnology Co. (Taichung, Taiwan) and Mirae Biotech (Gyeonggi, Korea), respectively.

Preparation And Characterization Of PGA-4HGF
PGA-4HGF was prepared by the previously reported ionic gelation method with appropriate modifications.[9] First, crude 4HGF was filtered through the filter paper

(Whatman's No. 1) and then centrifuged at 1,630 *g* for 10 min (Union 32R; Hanil Science Industrial Co., Incheon, Korea) to obtain the supernatant. Thereafter, the supernatant containing 4HGF was thoroughly mixed with PGA solution (1 mg/mL in water), followed by dropwise addition into aqueous CS solution [1 mg/mL in acetic acid (1%)] at room temperature with stirring for 1 h. During the synthesis reactions, several different volumetric ratios of PGA, CS, and 4HGF were used to investigate their effects on the nanoparticles. Following this, the prepared hydrogel nanoparticles were collected via centrifugation at 10,000 *g* for 10 min, washed three times with distilled water, and then dispersed in distilled water at 4°C until further use. PGA-control nanoparticles without 4HGF were prepared following the same procedures but distilled water was used instead of the 4HGF solution.

The size and morphology of the prepared nanoparticles were analyzed by transmission electron microscopy (TEM) and scanning electron microscopy (SEM) using the Jeol EM-2010 microscope (Jeol Co.) and Magellan 400 microscope (FEI Co.), respectively. For TEM analyses, 5 µL of the aqueous suspension of hydrogel nanoparticles was dropped on a copper TEM grid coated with

carbon (Electron Microscopy Sciences) and dried overnight at room temperature. Samples for SEM were prepared by placing a drop of suspension on polished wafer and air drying overnight at room temperature. Hydrodynamic size distribution and zeta potential analyses were carried out using a Zetasizer Nano-ZS (Malvern Co.).

Encapsulation Efficiency And Loading Capacity Of 4HGF Within PGA-4HGF

PGA-4HGF was characterized by determining its encapsulation efficiency (percentage of 4HGF encapsulated within PGA-4HGF compared with the initial amount of 4HGF) and loading capacity (percentage of 4HGF encapsulated within PGA-4HGF compared with total dry mass of hydrogel) as described earlier.[22] The amount of 4HGF entrapped within PGA-4HGF was measured by calculating the difference between the initially used amount and the amount of 4HGF that remained in the aqueous solution after the formation of PGA-4HGF. Determination of the amount of 4HGF was carried out by measuring the absorption intensity with a microplate reader (Synergy H1; BioTek, VT) in scanning mode or at 400 nm, which is the absorption wavelength of 4HGF.

In Vitro Release Study

Time-dependent release experiments were carried out by incubating PGA-4HGF (5 mg) in 10 mL of three different release media [sodium acetate (0.1 M, pH 4.0), PBS (pH 7.4), and sodium acetate (0.1 M, pH 5.5)] at 37°C or RT with agitation (150 rpm). At predetermined time intervals, 500 µL aliquots of both release media were withdrawn, and replaced immediately with the same volume of freshly prepared media. The aliquots were applied to the centrifugation at 10,000 g for 5 min to exclude the effects of hydrogel nanoparticles. Determination of the amount of 4HGF released from PGA-4HGF was performed by measuring the absorbance intensities of the supernatant as described above.

Evaluation Of Thermal Stabilities Via Antioxidant Activity Measurements

As free 4HGF as well as PGA-4HGF retain antioxidant activity, their thermal stabilities were evaluated by incubating them in distilled water under static conditions over a range of temperatures (4°C, 22°C, 37°C, 40°C, 50°C, 60°C, 70°C, and 80°C) for 5 h, and then their antioxidant activities were measured using DPPH radical scavenging
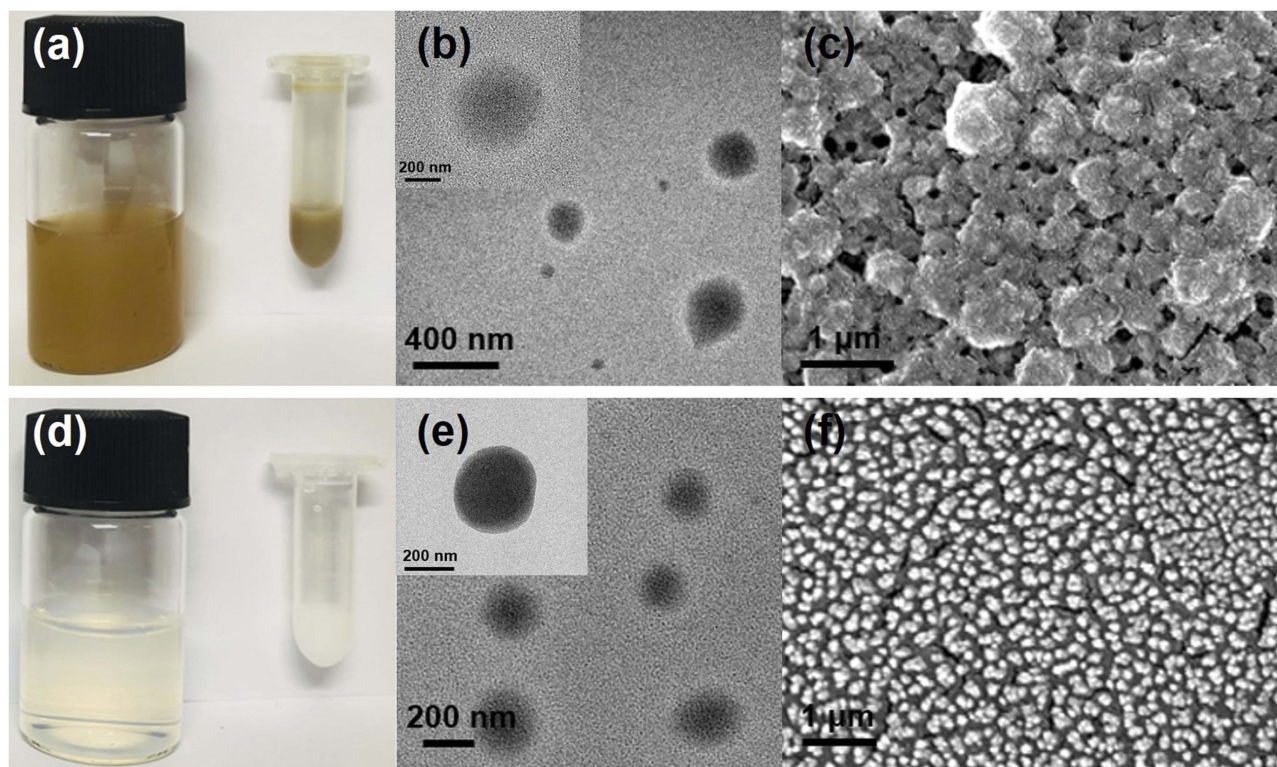

Figure 2 (**A**) Real image, (**B**) TEM image, and (**C**) SEM image of PGA-4HGF, and (**D**) real image, (**E**) TEM image, and (**F**) SEM image of PGA-control without 4HGF.

method.[23] In brief, 0.3 mL of each test sample was mixed with 0.2 mL DPPH stock solution (0.25 mM) in ethanol to produce a final DPPH concentration of 0.1 mM, and then allowed to react in the dark for 20 min. After the DPPH radical scavenging reaction, the absorbance was measured at 517 nm with a spectrophotometer (Varian, Palo Alto, CA). Ascorbic acid was used as the reference standard and all experiments were performed in triplicate. The percent DPPH radical scavenging activity was calculated using the ratio of the difference between the absorbance of reference and test sample to the absorbance of reference sample.

Evaluation Of Penetrating Efficiency Through Porcine Skin Using FITC-Labeled PGA-4HGF

To evaluate the penetrating efficiency of PGA-4HGF through the porcine skin, FITC-labeled CS was first synthesized according to a previously reported method with minor modifications.[24,25] Briefly, CS and FITC were dissolved to 1 mg/mL in 1% acetic acid solution and 1% methanol, respectively, followed by their slow mixing to 1:1 volumetric ratio to induce conjugation between the isothiocyanate group of FITC and the primary amine group of CS. After a 1-h reaction in the dark at room temperature, 0.1 M NaOH solution was added to precipitate FITC-labeled CS. The precipitate was excessively washed with distilled water until there was no FITC-driven green fluorescence in the washing solution. The FITC-labeled CS was then lyophilized using a freeze dryer (FDU-1200, EYELA, Japan). FITC-labeled CS was employed, rather than CS, for the synthesis of PGA-4HGF, as described above.

Porcine back skin was purchased from Cronex (Seoul, Korea) and used as a model to investigate the skin penetrating efficiency of the prepared fluorescent PGA-4HGF. The prepared FITC-labeled PGA-4HGF was rubbed twice a second on the skin followed by maintaining without any force for 10 s, to analyze their penetration ability under either static or shaking condition (150 rpm with shaking incubator [SI-7820, Optima, Japan]). At a predetermined time, we removed the residual nanoparticles on the porcine skin through several washing steps, and fixed the skin with 4% formaldehyde solution. The respective fluorescence from the FITC-labeled nanoparticles penetrating into the
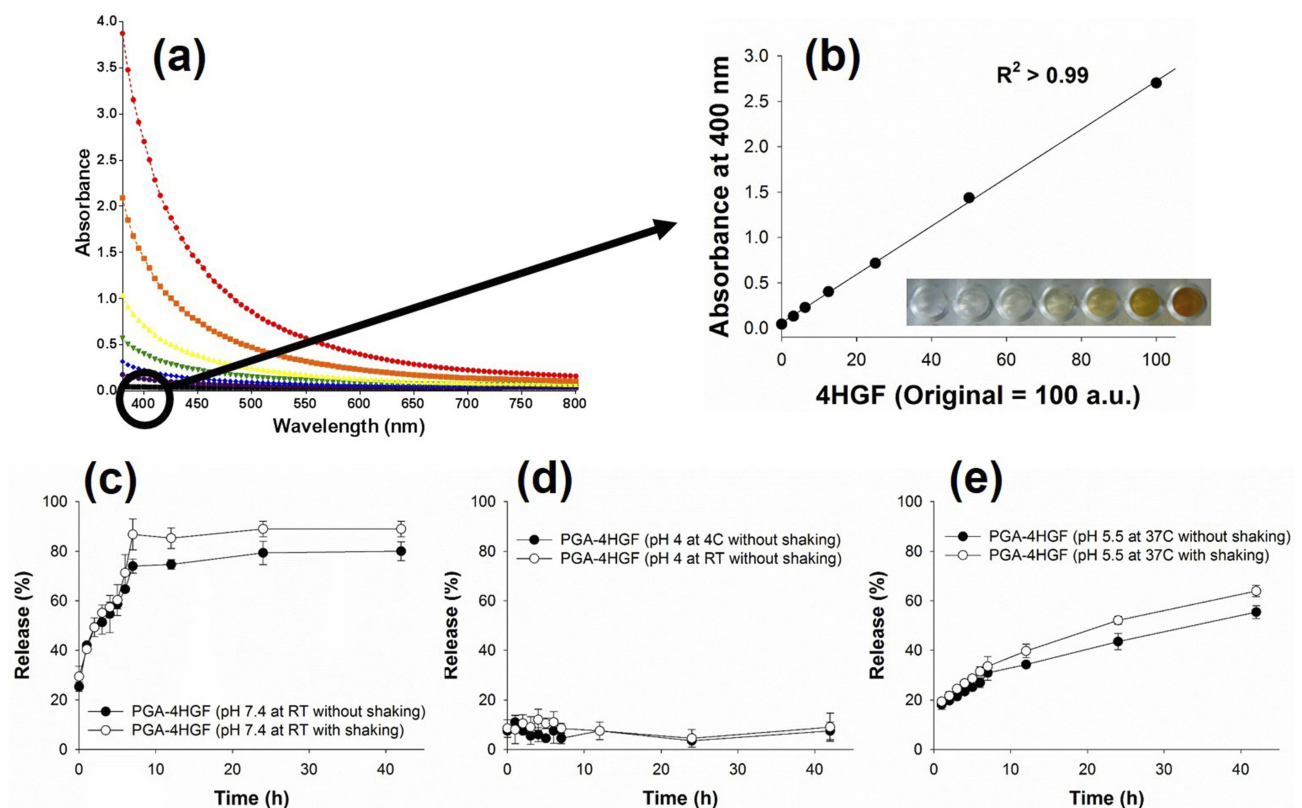

Figure 3 (**A**) Absorbance spectra of free 4HGF and (**B**) the corresponding standard curve of the concentration of 4HGF and absorption intensity measured at 400 nm. Release profiles of PGA-4HGF at (**C**) pH 7.4, (**D**) pH 4.0, and (**E**) hair follicles-like conditions (pH 5.5 & 37°C).

porcine skin was monitored using a confocal laser microscope system, excited by a 488 nm laser and detected using a 590/50 nm band pass filter.

Evaluation Of The Morphological Changes In DPCs

Primary DPCs were isolated from the hair bulbs of C57BL/6N mice, and cultured as previously described.[26] Cells (1×10^4 cells/well) were seeded in a 96-well plate and then incubated in the presence or absence of 5% (v/v) PGA-4HGF, PGA-control without 4HGF, or free 4HGF, dissolved in cell culture media. The applied concentration is calculated based on the volume of original 4HGF solution, which is either encapsulated within PGA-based hydrogel or free solution. Images were captured after 24 and 48 h of incubation using a Nikon Eclipse Ti microscope (Tokyo, Japan).

Evaluation Of The Size Of Hair Bulbs In C57BL/6N Mice

C57BL/6N telogenic mice (female; 7-week-old) were purchased from Orient Bio (Eumseong, Korea) and maintained in a 12 h light/dark cycle under specific pathogen-free conditions. Mice were randomly divided into four groups and provided with a standard diet. Dorsal skin (3×4 cm^2) were shaved using hair removal cream (BIKIRO cream, thioglycolic acid 80%; Tai Guk Pharm. Co. Ltd., Gyeonggi, Korea) as previously described.[26] Next, the shaved dorsal skin was treated with 200 μL of samples (distilled water (DW), PGA-control without 4HGF, PGA-4HGF, and free 4HGF) for 12 days. At day 12, the regrown hair were randomly plucked and measured for size (n > 10 hairs/mouse). The images of regrown hair were taken using a Nikon Eclipse Ti microscope (Tokyo, Japan). The size of the hair bulbs was measured using the MetaMorph program. This animal experiment was performed in accordance with the Institutional Animal Care and Use Committee (IACUC) Guidelines at Gachon University (GIACUC-R2016022, Gyeonggi, Seongnam, Korea).

Results And Discussion

The fabrication of PGA-4HGF began with thoroughly mixing 4HGF with PGA, followed by their dropwise addition into CS solution, resulting in quick formation of ~400 nm-sized spherical hydrogels. The photographic images of the synthesized hydrogel nanoparticles with or without 4HGF, as well as their size and morphology analyzed by TEM and SEM, were compared (Figure 2). As 4HGF is dark brown in

Table I (a) Effect Of Mixing Ratio Of PGA, 4HGF, And CS Or Mg^{2+} On The Synthesis Of Hydrogel Nanoparticles. (b) Effects Of CS Concentrations On The Synthesis Of Hydrogel Nanoparticles

(a)						
	Mixing Ratio (PGA: 4HGF: CS or Mg^{2+})	**Size (nm)**	**Zeta Potential (mV)**	**PDI**	**Encapsulation Efficiency (%)**	**Loading Capacity (wt%)**
PGA/CS with 4HGF	1:1:2 1:1:4 1:1:8	387.8±4.3 381.8±2.4 400.2±6.7	16.99±1.23 19.48±1.91 22.18±1.16	0.250±0.01 0.255±0.02 0.274±0.01	49.5±2.2 51.4±1.9 40.2±2.4	6.2±0.5 11.7±0.8 13.1±0.9
PGA/Mg^{2+} with 4HGF	1:1:2 1:1:4 1:1:8	643.0±7.7 565.4±8.8 541.4±10.7	−38.75±0.25 −38.75±0.25 −20.02±3.02	0.130±0.03 0.224±0.03 0.140±0.03	26.7±1.8 26.0±1.7 24.2±2.0	<2 <2 <2
PGA/CS-control without 4HGF	1:2 1:4	250±30.8 280±30.4	12.15±8.91 52.49±1.49	0.156±0.035 0.005±0.01	NA NA	NA NA
(b)						
CS (mg/mL) (Mixing Ratio = 1:1:4)		**Size (nm)**	**Zeta Potential (mV)**	**PDI**	**Encapsulation Efficiency (%)**	**Loading Capacity (wt%)**
0.1 0.2 0.5		153.2±3.8 176.4±10.8 222.4±6.7	−10.08±1.78 −2.74±0.66 3.46±0.64	0.250±0.01 0.255±0.02 0.292±0.01	2.1±0.2 2.5±0.1 4.7±0.1	<2 <2 <2

Abbreviation: NA, not applicable.

color, PGA-4HGF also appeared brownish (Figure 2A), whereas PGA-control without 4HGF appeared light white in color (Figure 2D), originating from the gel matrices only. Although it is relatively difficult to correctly visualize hydrogels by TEM and SEM analyses due to their water evaporation during the sample preparation and analyses,[8,27,28] we could observe approximately 400 nm-sized spherical particles of PGA-4HGF, which might have a higher content of gel matrices with less water content. Interestingly, smaller-sized (~300 nm) PGA-control particles were seen, indicating that the entrapment of 4HGF may enlarge the size of the nanoparticles. It has been reported that the transfollicular penetration of nanoparticles was largely affected by their size, and the nanoparticles sized at about 300–600 nm penetrated effectively with penetration depths proportional to their size.[29] PGA-4HGF also displayed a relatively rough surface with

aggregation and irregular sizes, whereas PGA-control without 4HGF was in a relatively in well-distributed state with a smooth surface, presumably due to the fact that there are many salt ingredients in 4HGF, possibly causing aggregation and irregular patterns in the hydrogel nanoparticles.

As it is difficult to identify a specific marker to quantify 4HGF,[21] we utilized the specific absorbance measured at 400 nm to produce a calibration plot of 4HGF (Figure 3A and B). Based on the standard curve, we determined the encapsulation efficiency and loading capacity of 4HGF, as well as the effect of diverse mixing ratios of PGA, 4HGF, and CS on the synthesis of the nanoparticles (Table 1). For further characterization, hydrodynamic size, surface zeta potential, and polydispersity index (PDI) were also analyzed. As shown in TEM images, the sizes of PGA-4HGF particles were determined to be ~400 nm, which were larger than
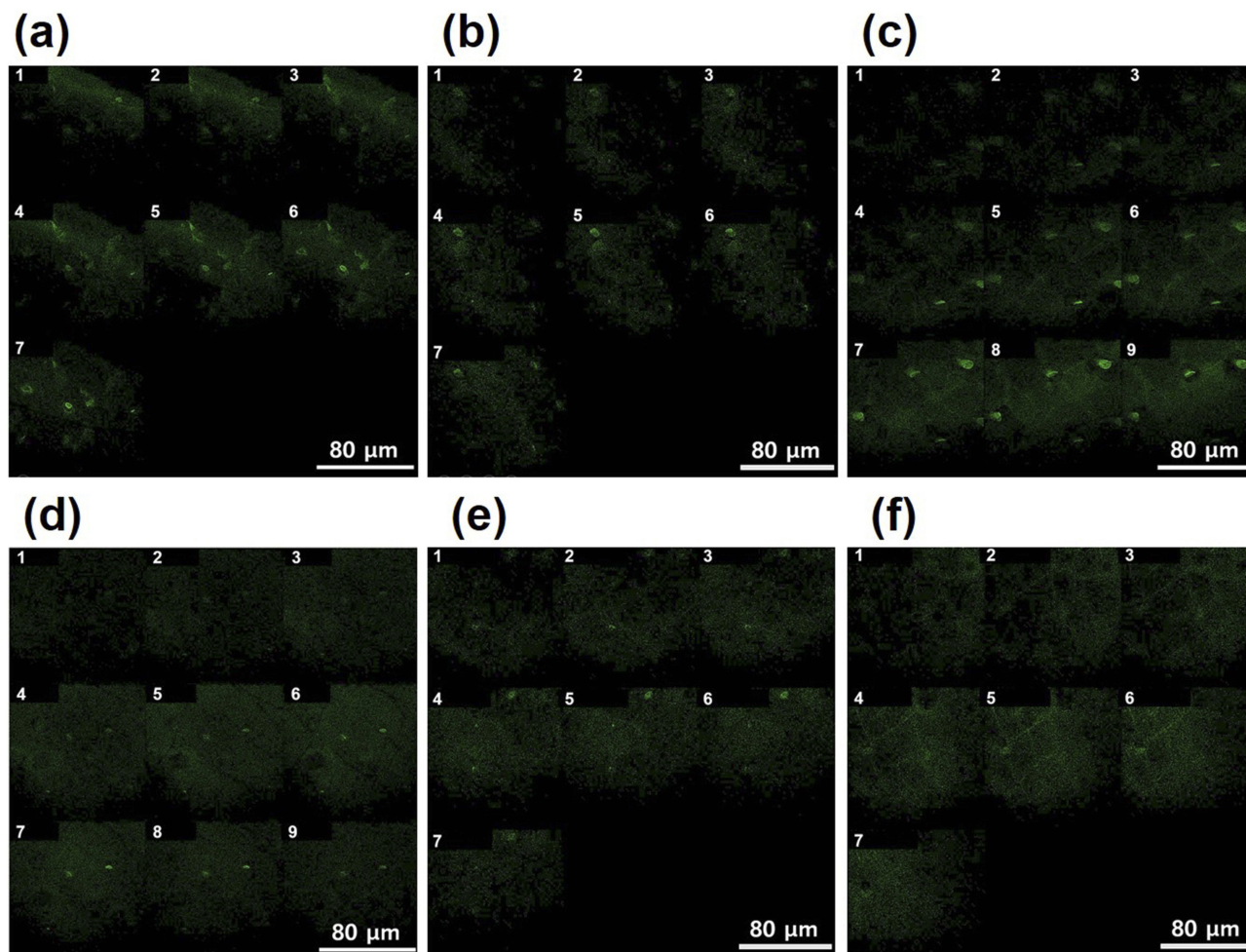

Figure 4 Penetration of FITC-labeled PGA-4HGF through the porcine skin after incubation with shaking (150 rpm) for (**A**) 0.5 hrs, (**B**) 3 hrs, and (**C**) 6 hrs, or without shaking for (**D**) 0.5 hrs, (**E**) 3 hrs, and (**F**) 6 hrs. Depth specifications: (**A**) 1: 15 µm, 2: 35 µm, 3: 85 µm, 4: 135 µm, 5: 185 µm, 6: 235 µm, and 7: 285 µm. (**B**) 1: 830 µm, 2: 860 µm, 3: 890 µm, 4: 950 µm, 5: 980 µm, 6: 1010 µm, and 7: 1070 µm. (**C**) 1: 1600 µm, 2: 1650 µm, 3: 1700 µm, 4: 1750 µm, 5: 1800 µm, 6: 1850 µm, 7: 1900 µm, 8: 1950 µm, and 9: 2000 µm. (**D**) 1: 0 µm, 2: 50 µm, 3: 100 µm, 4: 150 µm, 5: 200 µm, 6: 250 µm, 7: 300 µm, 8: 350 µm, and 9: 400 µm. (**E**) 1: 720 µm, 2: 750 µm, 3: 780 µm, 4: 840 µm, 5: 870 µm, 6: 900 µm, and 7: 960 µm. (**F**) 1: 910 µm, 2: 940 µm, 3: 970 µm, 4: 1030 µm, 5: 1060 µm, 6: 1090 µm, and 7: 1150 µm.

those of PGA-control without 4HGF, with acceptable PDI values (<0.3) to support mono-dispersed state with narrow size distributions.[30] The surface zeta potential was measured to be positive, possibly due to the cationic amine residues of CS. Because the highest encapsulation efficiency, greater than 50% of initially used 4HGF, was obtained with over 10 wt% loading capacity at a mixing ratio of 1:1:4 corresponding to PGA:4HGF:CS, this mixing ratio was chosen and used for further experiments. When magnesium ion was employed rather than CS, relatively larger-sized particles were observed with negative surface charges, and a critically lower encapsulation efficiency of below 30% with less than 2 wt% loading capacity was obtained due to inefficient preparation of the gel network. When lower CS concentrations (0.1, 0.2, and 0.5 mg/mL) were employed for the preparation of PGA-4HGF, lower values of encapsulation efficiency and loading capacity were obtained, as expected.

Time-dependent releases of encapsulated 4HGF were then investigated to examine the applicability of PGA-4HGF as delivery vehicles of 4HGF. As PGA/CS hydrogels have pH-dependent degradation characteristics,[9] 4HGF release was monitored under acidic (pH 4.0), physiological (pH 7.4), and hair follicles-like (pH 5.5 & 37°C) conditions.[31] At pH 7.4, 4HGF was rapidly released up to 7 h with or without shaking, while almost no release was observed at pH 4.0. Importantly, at hair follicles-like environments (pH 5.5 & 37°C), 4HGF was continuously released during 40 h incubation. These results indicate that the entrapped 4HGF was released at physiological and hair follicles-like pH conditions and efficiently preserved at acidic pH conditions (Figure 3C–E).

An excised human scalp is the best model to evaluate the penetrating efficiency of PGA-4HGF; however, there are ethical concerns regarding the use of human skin to evaluate percutaneous absorption, as well as relatively large variations among human skin samples due to differences in age, race, and anatomical donor site.[32] Thus, as a substitute for human scalp, we utilized porcine skin as a model to evaluate the penetrating efficiency of PGA-4HGF. Although there were many prescreening methods including radiotracer-based and electrochemical screening,[33–35] we just visually prescreened the skin and selected high-quality skin portion in this experiment. To track the penetration depth and speed at a given incubation time, FITC-labeled PGA-4HGF was prepared and applied on the porcine skin by rubbing, with or without shaking conditions. By observing the FITC-originated green fluorescence via confocal microscopy, our hydrogel nanoparticles clearly revealed their high penetrating speed and depth (Figure 4). Under

shaking condition, the penetration depth and speed after incubation for 6 h were approximately 2,000 μm and 333 μm/h, respectively. Under static condition, the penetration depth and speed after incubation for 6 h were roughly determined to be 1150 μm and 192 μm/h, respectively. Although studies using animal skin rather than human skin generally show more positive results for skin penetration,[36] our results suggest that PGA-4HGF might have the potential to be efficiently penetrated into the human skin or follicles, which is critical for enhancing the efficacy of hair growth-promoting agents.

Other advantages of PGA-4HGF include its enhanced stability and biodegradability. To assess stability, the antioxidant activities of the hydrogel nanoparticles entrapping 4HGF were determined along with those of free 4HGF (Figure 5A). For this, DPPH radical scavenging assay was employed.[23] The results show that PGA-4HGF as well as free 4HGF were stable even after incubation at 80°C for 5 h. This result is consistent with that of a previous study, which showed that free 4HGF itself is very stable due to its stable fermented extract components.[21] We next evaluated biodegradability of PGA-4HGF by measuring its size and PDI values after incubation in PBS buffer (pH 7.4). Results showed that the average size and PDI values increased with increasing incubation time, and the PDI value was higher than 0.3, suggesting that uniformity of particles was not maintained and diverse-sized particles were produced (Figure 5B).[30] This was presumably due to the time-dependent degradation of PGA-4HGF under physiological pH condition (pH 7.4), yielding disintegrated particles with large variations in their size distributions.[9]
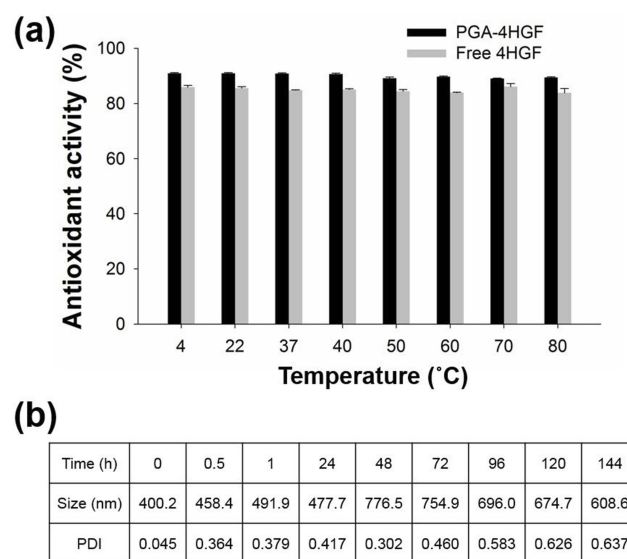

(a)

(b)

Time (h)	0	0.5	1	24	48	72	96	120	144
Size (nm)	400.2	458.4	491.9	477.7	776.5	754.9	696.0	674.7	608.6
PDI	0.045	0.364	0.379	0.417	0.302	0.460	0.583	0.626	0.637

Figure 5 (**A**) Thermal stability by DPPH radical scavenging activity assay. (**B**) Average size and PDI values of PGA-4HGF during incubation in PBS (pH 7.4).

In order to test the practical applicability of PGA-4HGF, telogenic mice and DPCs, which play an important role in the induction of hair growth by forming hair bulbs,[37–39] were treated with PGA-4HGF, and the results were compared with those of control treatment (PGA-control without 4HGF and free 4HGF). As expected, PGA-4HGF treatment yielded enlarged hair bulbs in mice compared to treatment with PGA-control without 4HGF or free 4HGF (Figure 6A). DPCs are multipotent hair follicle stem cells, which are stimulated to differentiate and proliferate during regrowth of hair

follicles.[40–42] It has also been reported that the morphology of stem cell-like DPCs is flattened and polygonal,[43] which is closely associated with the enlargement of hair bulb.[26,42,44,45] Thus, we investigated whether PGA-4HGF treatment induces morphological changes in primary DPCs. Results showed that a higher proportion of flattened and polygonal-shaped DPCs was observed in the PGA-4HGF-treated group than the control groups (Figure 6B). These results clearly indicate that PGA-4HGF caused enlargement of hair bulbs, possibly due to induction of DPCs with stem cell-like morphology.
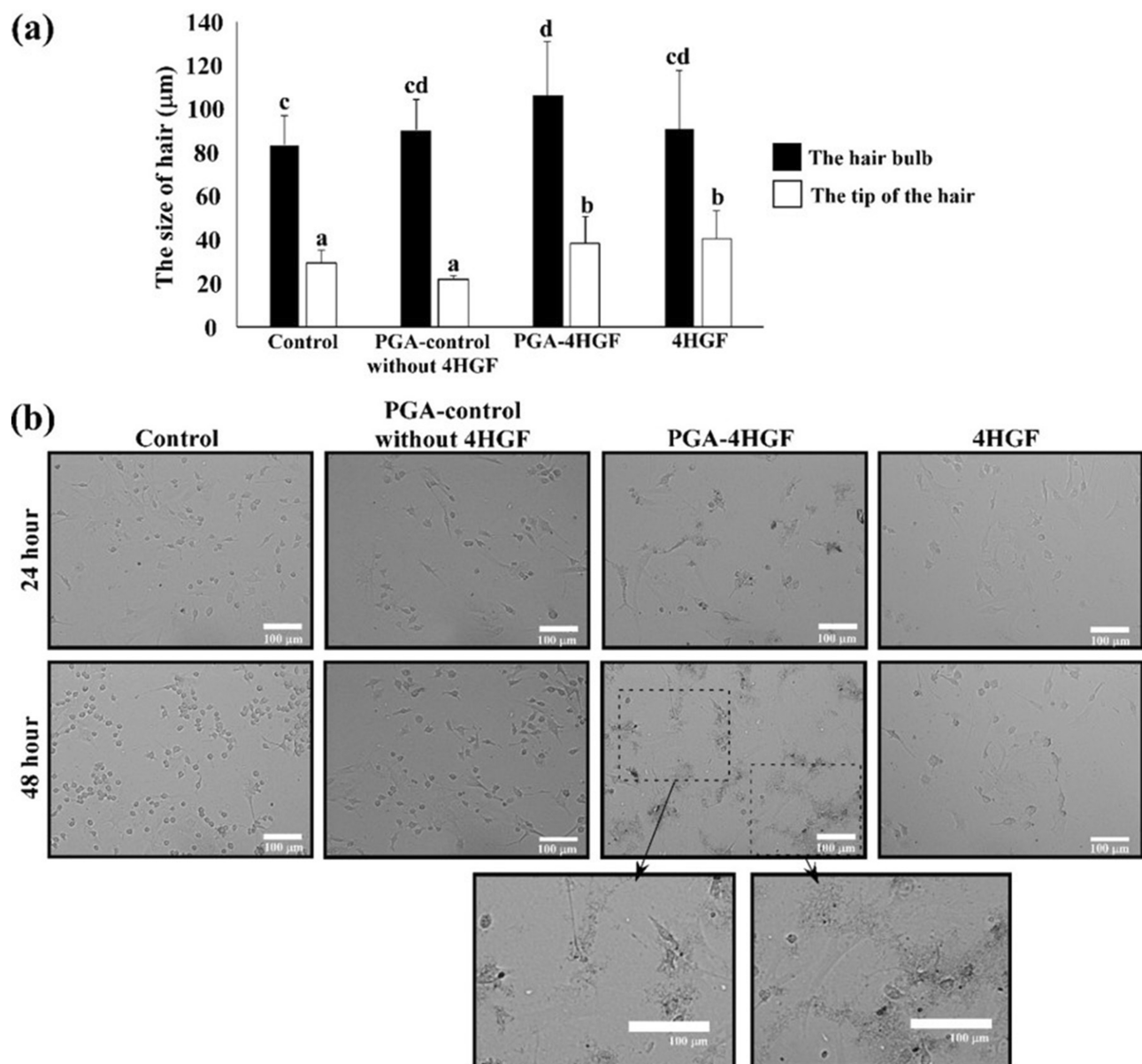

Figure 6 Effects of PGA-4HGF on: (**A**) the size of hair bulbs in mice and (**B**) the morphology of DPCs. In (**A**), data are represented as mean ± standard deviation (SD) (n > 30 hairs), and values with different alphabets in the same row were significantly different. Scale bar = 100 µm. Data were analyzed by one-way analysis of variance (ANOVA)/Duncan's t-test. ($p < 0.05$).

Conclusion

We herein fabricated PGA-4HGF nanoparticles for their effective delivery into hair follicles to promote hair growth. The results of this study demonstrated that the hydrogel nanoparticles enabled high encapsulation efficiency and loading capacity for 4HGF, sustained release in physiological pH environments, efficient penetration through the model porcine skin, and time-dependent degradation under physiological conditions. Finally, application of PGA-4HGF successfully enlarged the hair bulb of mice by inducing morphological changes in DPCs. As this new hydrogel formulation has the potential to deliver hair growth-promoting compounds more efficiently into hair follicles, it can be potentially utilized in the field of hair-care cosmeceuticals. Further studies demonstrating the mechanisms underlying promotion of hair growth,[26] as well as human testing are underway in our group, with an aim to launch new PGA-4HGF-based hair growth-promoting products in the market.

Disclosure

The authors report no conflicts of interest in this work.

References

1. Kaul S, Gulati N, Verma D, Mukherjee S, Nagaich U. Role of nanotechnology in cosmeceuticals: a review of recent advances. *J Pharm*. 2018;3420204:1–19. doi:10.1155/2018/3420204
2. Mu L, Sprando RL. Application of nanotechnology in cosmetics. *Pharm Res*. 2010;27:1746–1749. doi:10.1007/s11095-010-0139-1
3. Zhang L, Ma YN, Pan XC, Chen SY, Zhuang HH, Wang SF. A composite hydrogel of chitosan/heparin/poly (gamma-glutamic acid) loaded with superoxide dismutase for wound healing. *Carbohydr Polym*. 2018;180:168–174. doi:10.1016/j.carbpol.2017.10.036
4. Zohuriaan-Mehr MJ, Pourjavadi A, Salimi H, Kurdtabar M. Protein- and homo poly(amino acid)-based hydrogels with super-swelling properties. *Polym Adv Technol*. 2009;20:655–671. doi:10.1002/pat.1395
5. Kong M, Chen XG, Xing K, Park HJ. Antimicrobial properties of chitosan and mode of action: a state of the art review. *Int J Food Microbiol*. 2010;144:51–63. doi:10.1016/j.ijfoodmicro.2010.09.012
6. Malik A, Gupta M, Gupta V, Gogoi H, Bhatnagar R. Novel application of trimethyl chitosan as an adjuvant in vaccine delivery. *Int J Nanomed*. 2018;13:7959–7970. doi:10.2147/IJN.S165876
7. Malik A, Gupta M, Mani R, Gogoi H, Bhatnagar R. Trimethyl chitosan nanoparticles encapsulated protective antigen protects the mice against anthrax. *Front Immunol*. 2018;9:562. doi:10.3389/fimmu.2018.00562
8. Lin YH, Chung CK, Chen CT, Liang HF, Chen SC, Sung HW. Preparation of nanoparticles composed of chitosan/poly-gamma-glutamic acid and evaluation of their permeability through Caco-2 cells. *Biomacromolecules*. 2005;6:1104–1112. doi:10.1021/bm049312a
9. Sonaje K, Chen YJ, Chen HL, et al. Enteric-coated capsules filled with freeze-dried chitosan/poly (γ-glutamic acid) nanoparticles for oral insulin delivery. *Biomaterials*. 2010;31:3384–3394. doi:10.1016/j.biomaterials.2010.01.042
10. Tang DW, Yu SH, Ho YC, Mi FL, Kuo PL, Sung HW. Heparinized chitosan/poly (γ-glutamic acid) nanoparticles for multi-functional delivery of fibroblast growth factor and heparin. *Biomaterials*. 2010;31:9320–9332. doi:10.1016/j.biomaterials.2010.08.058
11. Chen Y, Yan XT, Zhao JA, et al. Preparation of the chitosan/poly (glutamic acid)/alginate polyelectrolyte complexing hydrogel and study on its drug releasing property. *Carbohydr Polym*. 2018;191:8–16. doi:10.1016/j.carbpol.2018.02.065
12. Lohani A, Verma A, Joshi H, Yadav N, Karki N. Nanotechnology-based cosmeceuticals. *ISRN Dermatol*. 2014;843687:1–14. doi:10.1155/2014/843687
13. Baswan S, Kasting GB, Li SK, et al. Understanding the formidable nail barrier: a review of the nail microstructure, composition and diseases. *Mycoses*. 2017;60:284–295. doi:10.1111/myc.12592
14. Fang CL, Aljuffali IA, Li YC, Fang JY. Delivery and targeting of nanoparticles into hair follicles. *Ther Deliv*. 2014;5:991–1006. doi:10.4155/tde.14.61
15. Daniells S, Hardy G. Hair loss in long-term or home parenteral nutrition: are micronutrient deficiencies to blame? *Curr Opin Clin Nutr Metab Care*. 2010;13:690–697. doi:10.1097/MCO.0b013e32833ece02
16. Kang JI, Kim MK, Lee JH, et al. Undariopsis petersenina promotes hair growth by the activation of Wnt/beta-Catenin and ERK pathways. *Mar Drugs*. 2017;15:130. doi:10.3390/md15050130
17. Cotsarelis G, Millar SE. Towards a molecular understanding of hair loss and its treatment. *Trends Mol Med*. 2001;7:293–301. doi:10.1016/S1471-4914(01)02027-5
18. Messenger AG, Rundegren J. Minoxidil: mechanisms of action on hair growth. *Br J Dermatol*. 2004;150:186–194. doi:10.1111/j.1365-2133.2004.05785.x
19. Georgala S, Befon A, Maniatopoulou E, Georgala C. Topical use of minoxidil in children and systemic side effects. *Dermatol*. 2007;214:101–102. doi:10.1159/000096924
20. Li Y, Han M, Lin P, He YR, Yu J, Zhao RH. Hair growth promotion activity and its mechanism of polygonum multiflorum, evid based complement. *Alternat Med*. 2015;517901:1–10. doi:10.1155/2015/517901
21. Park HJ, Zhang N, Park DK. Topical application of polygonum multiflorum extract induces hair growth of resting hair follicles through upregulating shh and beta-catenin expression in C57BL/6 mice. *J Ethnopharmacol*. 2011;135:369–375. doi:10.1016/j.jep.2011.03.028
22. Zhang ZP, Feng SS. The drug encapsulation efficiency, in vitro drug release, cellular uptake and cytotoxicity of paclitaxel-loaded poly(lactide)-tocopheryl polyethylene glycol succinate nanoparticles. *Biomaterials*. 2006;27:4025–4033. doi:10.1016/j.biomaterials.2006.03.006
23. Pyrzynska K, Pekal A. Application of free radical diphenylpicrylhydrazyl (DPPH) to estimate the antioxidant capacity of food samples. *Anal Methods*. 2013;5:4288–4295. doi:10.1039/C3AY40367J
24. Peng SF, Yang MJ, Su CJ, et al. Effects of incorporation of poly (γ-glutamic acid) in chitosan/DNA complex nanoparticles on cellular uptake and transfection efficiency. *Biomaterials*. 2009;30:1797–1808. doi:10.1016/j.biomaterials.2008.12.019

25. Qaqish R, Amiji M. Synthesis of a fluorescent chitosan derivative and its application for the study of chitosan–mucin interactions. *Carbohydr Polym*. 1999;38:99–107. doi:10.1016/S0144-8617(98)00109-X

26. Lee HJ, Kwon HK, Kim HS, Kim MI, Park HJ. Hair growth promoting effect of 4HGF encapsulated with PGA nanoparticles (PGA-4HGF) by β-catenin activation and its related cell cycle molecules. *Int J Mol Sci*. 2019;20:3447. doi:10.3390/ijms20143447

27. Liu Y, Chen X, Li S, et al. Calcitonin-loaded thermosensitive hydrogel for long-term antiosteopenia therapy. *ACS Appl Mater Inter*. 2017;9:23428–23440. doi:10.1021/acsami.7b05740

28. Abandansari HS, Aghaghafari E, Nabid MR, Niknejad H. Preparation of injectable and thermoresponsive hydrogel based on penta-block copolymer with improved sol stability and mechanical properties. *Polymer*. 2013;54:1329–1340. doi:10.1016/j.polymer.2013.01.004

29. Sahle FF, Giulbudagian M, Bergueiro J, Lademann J, Calderon M. Dendritic polyglycerol and N-isopropylacrylamide based thermoresponsive nanogels as smart carriers for controlled delivery of drugs through the hair follicle. *Nanoscale*. 2017;9:172–182. doi:10.1039/c6nr06435c

30. Sadeghi R, Etemad SG, Keshavarzi E, Haghshenasfard M. Investigation of alumina nanofluid stability by UV-vis spectrum. *Microfluid Nanofluidics*. 2015;18:1023–1030. doi:10.1007/s10404-014-1491-y

31. Dimde M, Sahle FF, Wycisk V, et al. Synthesis and validation of functional nanogels as pH-sensors in the hair follicle. *Macromol Biosci*. 2017;17:1600505. doi:10.1002/mabi.201700070

32. Todo H. Transdermal permeation of drugs in various animal species. *Pharmaceutics*. 2017;9:33. doi:10.3390/pharmaceutics9030033

33. Baswan SM, Leverett J, Pawelek J. Clinical evaluation of the lightening of cytidine on hyperpigmented skin. *J Cosmet Dermatol*. 2019;18:278–285. doi:10.1111/jocd.12784

34. Baswan SM, Li SK, LaCount TD, Kasting GB. Size and charge dependence of ion transport in human nail plate. *J Pharm Sci*. 2016;105:1201–1208. doi:10.1016/j.xphs.2015.12.011

35. Baswan SM, Li SK, Kasting GB. Diffusion of uncharged solutes through human nail plate. *Pharm Dev Technol*. 2016;21:255–260. doi:10.3109/10837450.2014.991876

36. Labouta HI, Schneider M. Interaction of inorganic nanoparticles with the skin barrier: current status and critical review. *Nanomedicine*. 2013;9:39–54. doi:10.1016/j.nano.2012.04.004

37. Lai-Cheong JE, McGrath JA. Structure and function of skin, hair and nails. *Medicine*. 2017;45:347–351. doi:10.1016/j.mpmed.2009.03.002

38. Roth SI, Helwig EB. The cytology of the dermal papilla, the bulb, and the root sheaths of the mouse hair. *J Ultrastruct Res*. 1964;11:33–51. doi:10.1016/S0022-5320(64)80091-5

39. Bae S, Kim J, Li L, et al. Canine adipose-derived stem cell aggregates as a viable substitute to actual canine dermal papillae. *Mac Vet Rev*. 2015;38:167–173. doi:10.14432/j.macvetrev.2015.05.043

40. Roh C, Tao Q, Lyle S. Dermal papilla-induced hair differentiation of adult epithelial stem cells from human skin. *Physiol Genomics*. 2004;19:207–217. doi:10.1152/physiolgenomics.00134.2004

41. Rendl M, Polak L, Fuchs E. BMP signaling in dermal papilla cells is required for their hair follicle-inductive properties. *Genes Dev*. 2008;22:543–557. doi:10.1101/gad.1614408

42. Kiratipaiboon C, Tengamnuay P, Chanvorachote P. Glycyrrhizic acid attenuates stem cell-like phenotypes of human dermal papilla cells. *Phytomedicine*. 2015;22:1269–1278. doi:10.1016/j.phymed.2015.11.002

43. Bratka-Robia CB, Mitteregger G, Aichinger A, Egerbacher M, Helmreich M, Bamberg E. Primary cell culture and morphological characterization of canine dermal papilla cells and dermal fibroblasts. *Vet Dermatol*. 2002;13:1–6. doi:10.1046/j.0959-4493.2001.00276.x

44. Osada A, Iwabuchi T, Kishimoto J, Hamazaki TS, Okochi H. Long-term culture of mouse vibrissal dermal papilla cells and de novo hair follicle induction. *Tissue Eng*. 2007;13:975–982. doi:10.1089/ten.2006.0304

45. Yoo BY, Shin YH, Yoon HH, Seo YK, Park JK. Hair follicular cell/organ culture in tissue engineering and regenerative medicine. *Biochem Eng J*. 2010;48:323–331. doi:10.1016/j.bej.2009.09.008